Modulation of Reactive Oxygen Species in Pancreatic Cancer

Melissa L.T. Teoh,[2] Wenqing Sun,[2] Brian J. Smith,[3] Larry W. Oberley,[2,3] and Joseph J. Cullen[1,2,3,4]

Abstract

Purpose: The aim of the present study was to compare the effects of the three different forms of the antioxidant enzyme superoxide dismutase [i.e., manganese superoxide dismutase (MnSOD), copper zinc superoxide dismutase (CuZnSOD), and extracellular superoxide dismutase (EcSOD)] on the malignant phenotype of human pancreatic cancer.

Experimental Design: Human pancreatic cancer cell lines were infected with adenoviral vectors containing the cDNAs for three different forms of the antioxidant enzyme SOD. Intratumoral injections of the adenoviral vectors were used in nude mice with human tumor xenografts.

Results: Increases in immunoreactive protein and enzymatic activity were seen after infections with the Ad*MnSOD*, Ad*CuZnSOD*, or Ad*EcSOD* constructs. Increased SOD activity decreased superoxide levels and increased hydrogen peroxide levels. Increasing SOD levels correlated with increased doubling time. Cell growth and plating efficiency decreased with increasing amounts of the adenoviral constructs, with the Ad*CuZnSOD* vector having the greatest effect in decreasing *in vitro* tumor growth. In contrast, inhibiting endogenous SOD with small interfering RNA increased superoxide levels and promoted tumor growth. Of the three SODs, tumors grew the slowest and survival was increased the greatest in nude mice injected with the Ad*EcSOD* construct.

Conclusions: Scavenging plasma membrane–generated superoxide may prove beneficial for suppression of pancreatic cancer growth.

Adenocarcinoma of the pancreas is the fourth leading cause of cancer death in the United States and is increasing in incidence (1). K-*ras* mutations have been identified in up to 95% of pancreatic cancers, implying their critical role in the molecular pathogenesis (2–4). It is hypothesized that K-*ras* activates the NADPH oxidase system to produce reactive oxygen species (ROS) that leads to cell proliferation (5). Vaquero et al. (5) have recently shown that ROS are prosurvival, antiapoptotic factors in pancreatic cancer. They showed that growth factors stimulate ROS generation by activation of membrane non-mitochondrial NAD(P)H oxidase and that inhibiting ROS by different approaches stimulates apoptosis in pancreatic cancer cells. Thus, the prosurvival effect of ROS may be an important mechanism of pancreatic cancer cell resistance to therapy. Santillo et al. (6) added to these findings by showing that in K-*ras*–transformed mouse fibroblasts, ROS are increased, leading to activation of signal transduction pathways. In addition to K-*ras*, mouse fibroblasts transfected with the viral Ha-*ras* oncogene have increased superoxide (O_2^-) production and the generated O_2^- may act as a second messenger molecule to promote cell proliferation (7). Similar results have been found in human keratinocytes with Ha-*ras* (8). In *ras*-transformed keratinocytes, increased O_2^- production was shown, and this increased production could be blocked efficiently by an adenovirus containing the cDNA of the antioxidant protein superoxide dismutase (SOD; ref. 8).

Cells contain a large number of antioxidants to prevent or repair the damage caused by ROS. The SODs dismutate O_2^- into H_2O_2, whereas the catalases and peroxidases convert H_2O_2 into water. In this way, two toxic species, O_2^- and H_2O_2, are converted to the harmless product water. An important feature of these enzymes is that they are highly compartmentalized (9). In general, extracellular superoxide dismutase (EcSOD) is the only isoform of SOD that is expressed extracellularly; manganese-containing superoxide dismutase (MnSOD) is localized in the mitochondria; and copper- and zinc-containing superoxide dismutase (CuZnSOD) is expressed in the cytoplasm. One reason for the existence of many forms of each of these enzymes is to reduce oxidative stress in the various parts of the cell; different proteins are needed for different cellular and subcellular locations. CuZnSOD comprises ~90% of total SOD activity in most eukaryotic cells (10). Besides its primary distribution in cytosol, a small fraction of this enzyme has been found in cellular organelles such as lysosomes, peroxisomes, and the nucleus. Recently, there has been some evidence showing the presence of CuZnSOD (~2%) in the intermembrane space of mitochondria (11, 12) and this localization was suggested to be important in providing further protection against ROS and in preventing superoxide radicals from leaking out of the mitochondria. Although EcSOD also uses copper as a

Authors' Affiliations: Departments of [1]Surgery and [2]Radiation Oncology, University of Iowa College of Medicine; [3]Holden Comprehensive Cancer Center; and [4]Veterans Affairs Medical Center, Iowa City, Iowa

Received 4/12/07; revised 6/27/07; accepted 7/3/07.

Grant support: NIH grants CA115785 and CA66081, the Medical Research Service, Department of Veterans Affairs, and the Susan L. Bader Foundation of Hope.

The costs of publication of this article were defrayed in part by the payment of page charges. This article must therefore be hereby marked *advertisement* in accordance with 18 U.S.C. Section 1734 solely to indicate this fact.

Requests for reprints: Joseph J. Cullen, 4605 JCP, University of Iowa Hospitals and Clinics, Iowa City, IA 52242. Phone: 319-353-8297/319-339-5497; Fax: 319-356-8378; E-mail: joseph-cullen@uiowa.edu.

doi:10.1158/1078-0432.CCR-07-0851

catalytic cofactor and zinc as a structural component in a similar fashion as CuZnSOD, the expression of EcSOD is highly restricted to specific cell types and tissues such as lung, heart, kidney, plasma, lymph, ascites, and cerebrospinal fluid (13). EcSOD is the only isoform of SOD that is expressed extracellularly (14, 15). A fundamental property of EcSOD is its affinity, through its heparin-binding domain, for heparin sulfate proteoglycans located on cell surfaces and in extracellular matrix (16). In addition, EcSOD differs from CuZnSOD in that EcSOD is a glycosylated high molecular weight homotetramer (155 kDa) and CuZnSOD is an unglycosylated homodimer (32 kDa). Increasing EcSOD expression has been shown to inhibit the *in vitro* growth of melanoma tumors by blunting tumor vascularization and vascular endothelial growth factor expression (15). MnSOD is limited to the matrix of the mitochondria (17) and exists at much lower concentrations inside most cells than CuZnSOD. Because the mitochondrial respiratory chain is a major site of superoxide generation in cells, MnSOD plays an important role in maintaining the balance of cellular ROS. Our previous studies showed a tumor-suppressive effect of MnSOD on both *in vitro* and *in vivo* growth of pancreatic cancer (18, 19).

Because ROS generation by activation of membrane nonmitochondrial NAD(P)H oxidase seems to be one mechanism regulating cell growth contributing to pancreatic tumor progression, we hypothesized that scavenging of superoxide generated from the plasma membrane would also inhibit pancreatic cancer growth. Our studies confirm that overexpression of MnSOD inhibits pancreatic tumor growth (18, 19). In addition, we show that scavenging of superoxide with the antioxidant enzymes EcSOD and CuZnSOD has a stronger tumor-suppressive effect in pancreatic cancer than MnSOD.

Materials and Methods

Cell culture. Pancreatic cancer cells were purchased from American Type Culture Collection. MIA PaCa-2 cells are undifferentiated human primary pancreatic adenocarcinoma cells (18) and are maintained at 37°C in DMEM (Life Technologies, Inc.) supplemented with 10% heat-inactivated fetal bovine serum and 2.5% horse serum. BxPC-3 cells are poorly differentiated human primary pancreatic adenocarcinoma cells (18) and are maintained in RPMI 1640 with 10% fetal bovine serum.

Adenovirus gene transfer. The adenovirus constructs used were replication-defective, E1- and partial E3-deleted recombinant adenovirus (18, 19). Inserted into the E1 region of the adenovirus genome was the human *MnSOD*, *CuZnSOD*, or *EcSOD* gene, which is driven by a cytomegalovirus promoter. For the vector control, we used the same adenovirus with no gene added (an empty vector; Ad*Empty*). Both Ad*CuZnSOD* and Ad*EcSOD* constructs were obtained from the University of Iowa Gene Transfer Vector Core whereas the Ad*Empty* and Ad*MnSOD* constructs were purchased from ViraQuest.

Approximately 10^6 cells were plated in 10 mL of complete medium in a 90-cm^2 plastic dish and allowed to attach for 24 h. Cells were then washed thrice in serum- and antibiotic-free medium. The Ad*MnSOD*, Ad*CuZnSOD*, or Ad*EcSOD* constructs, suspended in 3% sucrose, were then applied to cells suspended in 4 mL of serum- and antibiotic-free medium at 0, 10, 25, 50, and 100 multiplicities of infection (MOI). Control cells were treated with 100 MOI of the Ad*Empty* construct. Cells were incubated with the adenovirus constructs for 24 h. Medium was then replaced with 10 mL of complete medium for an additional 24 h before cells were harvested.

RNA interference. Inhibition of CuZnSOD and MnSOD was achieved by using small interfering RNA (siRNA). Predesigned double-stranded siRNA against MnSOD (siMnSOD) was purchased from Ambion, Inc., with the sequence of 5′-GGCCUGAUUAUCUAAAAGCtt-3′. siRNA against CuZnSOD was custom designed using a computer program available from Ambion with the sequence of 5′-GGCCUGCAUGGAUUCCAUGtt-3′. As a negative control, a siNeg siRNA, verified to have no significant effect on most essential mammalian genes, was obtained from Ambion.

siRNA transfection. MIA PaCa-2 cells (1×10^6) were seeded into 60-mm plates with 4 mL of complete DMEM. After 24 h, the medium was replaced with 4 mL of Opti-MEM (Life Technologies). Cells were then transfected with 200 pmol of the siRNAs using LipofectAMINE 2000 reagent (Invitrogen) in accordance with the manufacturer's protocol. After 48 h of transfection, cells were trypsinized and reseeded into 24-well plates at a density of 5×10^3 per well. At different time points, cells were harvested to determine growth rates, antioxidant protein, and activity.

Cell lysis and protein determination. Cells were washed thrice in PBS (pH 7.0) and scrape harvested from the dishes using a rubber policeman. Cells were then lysed in NP40 lysis buffer [50 mmol/L Tris-HCl (pH 8.0), 120 mmol/L NaCl, 1% NP40, 5 mmol/L EDTA, and protease inhibitor cocktail tablet (Roche Diagnostics)] and protein concentration was determined using the Bio-Rad Bradford dye binding protein assay kit according to the manufacturer's instructions.

Western blot analysis. Immunoreactive protein corresponding to MnSOD, CuZnSOD, or EcSOD was identified and quantitated from total cell protein by the specific reaction of the immobilized protein with its antibody. Total protein was electrophoresed in a 12.5% SDS-polyacrylamide running gel and a 5% stacking gel. Actin was used for loading controls. The proteins were then electrotransferred onto nitrocellulose sheets. After blocking in 5% nonfat powdered milk for 1 h, the sheets were washed and then treated with antisera to MnSOD, CuZnSOD, or EcSOD (1:5,000) for overnight at 4°C. Antibodies to MnSOD and CuZnSOD have been prepared and characterized in our laboratory (18), whereas the EcSOD antibody was prepared and characterized by Dr. James Crapo (National Jewish Medical and Research Center, Denver, CO). The blot was incubated with horseradish peroxidase–conjugated goat anti-rabbit (Sigma) IgG (1:100,000) for 1 h at room temperature. The washed blot was then treated with SuperSignal West Pico Chemiluminescent substrate (Pierce) and exposed to X-ray film. Western blots were done in duplicate.

Antioxidant enzyme activity gels. Nondissociating slab gels were run essentially by the method of Davis (20) with ammonium persulfate used as the initiator in the running gel (12.5%) and riboflavin-light in the stacking gel (5%). Once run, the gels were stained for SOD activity by the method of Beauchamp and Fridovich (21). CuZnSOD and MnSOD were differentiated by the presence of sodium cyanide in the staining solution, which inhibits CuZnSOD. All antioxidant enzyme activity gels were done in duplicate.

Cell growth. After 48 h of adenoviral infection, cells were trypsinized, counted, and reseeded at a density of 1×10^4 in 24-well plates with 1.5 mL of complete medium. For the growth analysis, cells were trypsinized and then counted daily for 1 week using a Coulter counter. Cell population doubling time (DT) in hours was determined using the following equation:

$$\mathrm{DT\ (hours)} = 0.693\ (t - t_o)/\ln\ (N_t/N_o)$$

where t_o, time at which exponential growth began; t, time in hours; N_t, cell number at time t; and N_o, initial cell number (18).

Cell death measurements. Phosphatidylserine translocation to the outer leaflet of the plasma membrane was assessed by reaction with Annexin V-FITC and detected with a FACScan flow cytometer. MIA PaCa-2 cells (1×10^6) were infected with adenovirus constructs at 100 MOI. After 48 h, cells were harvested, washed with PBS, and resuspended in 500 μL of binding buffer [10 mmol/L HEPES (pH 7.4), 140 mmol/L NaCl, 2.5 mmol/L $CaCl_2$]. Cells were then incubated with

5 μL of Annexin V conjugated with FITC plus 5 μg/mL propidium iodide and incubated for 10 min at room temperature in the dark. Samples were then analyzed by flow cytometry to identify apoptotic and necrotic cells.

Measurement of ROS levels. Intracellular generation of $O_2^{\cdot}$ was assessed by hydroethidine fluorescence. The level of presumably intracellular peroxide was also determined with dichlorofluorescein (DCFH) diacetate (Molecular Probes, Inc.). In other experiments, to determine if increases in fluorescence of DCFH were due to hydrogen peroxide, cells were also treated with PEGylated catalase (PEG-catalase, Sigma), 100 units/mL for 2 h, before DCFH measurement. Briefly, cells were incubated with 10 μmol/L dihydroethidium or 10 μmol/L DCFH in complete medium for 40 min at 37°C with 5% CO_2. Cells were then washed with PBS and harvested. Cells were lysed with 1% SDS and the fluorescent intensity of dihydroethidium or DCFH in the lysate was assessed by using a microplate reader (SpectraFluor Plus, Tecan) with an excitation wavelength of 485 nm and emission wavelengths of 530 and 590 nm, respectively. The protein concentration of the lysate was determined by using the Bio-Rad Dc Protein assay and the ROS levels were expressed as mean fluorescent intensity per milligram of protein.

Plating efficiency. Ad*MnSOD*-, Ad*CuZnSOD*-, Ad*ECSOD*-, or Ad*Empty*-transduced cells (100 MOI) were plated in triplicate into 60-mm dishes in complete medium. The dishes were maintained in the incubator for 6 days to allow colony formation. The colonies were then fixed and stained with 0.1% crystal violet and 2.1% citric acid, and those colonies containing >50 cells were scored.

Nude mice. Thirty-day-old athymic nude mice were obtained from Harlan Sprague-Dawley. The nude mouse protocol was reviewed and approved by the Animal Care and Use Committee of the University of Iowa. The animals were housed four to a cage and fed a sterile commercial stock diet and tap water *ad libitum*. Animals were allowed to acclimate in the unit for 1 week before any manipulations were done. Each experimental group consisted of five to eight mice.

Adenovirus vector–mediated* MnSOD, CuZnSOD, *or* EcSOD *gene transfer. MIA PaCa-2 tumor cells (2×10^6) were delivered s.c. into the flank region of nude mice with a 1-mL tuberculin syringe equipped with a 25-gauge needle. The tumors were allowed to grow until they reached between 3 and 4 mm in greatest dimension (from 10 days to 2 weeks), at which time they were treated with adenovirus.

The adenovirus constructs were delivered through two injection sites in the tumor. Approximately 1×10^9 plaque-forming units in 50 μL of PBS of the Ad*MnSOD*, Ad*CuZnSOD*, or Ad*EcSOD* constructs were delivered to the tumor by means of a 25-gauge needle attached to a 1-mL tuberculin syringe. This was defined as day 1 of the experiment. Control tumors received serum-free media or adenovirus containing no gene (Ad*Empty*) in similar volumes and plaque-forming units at the same time points. Tumor size was measured every 2 to 3 days by means of a vernier caliper, and tumor volume was estimated according to the following formula: tumor volume = $\pi / 6 \times L \times W^2$, where L is the greatest dimension of the tumor and W is the dimension of the tumor in the perpendicular direction (19). Animals were killed by CO_2 asphyxiation when the tumors reached a predetermined size of 1,000 mm^3, and this was considered the time to sacrifice.

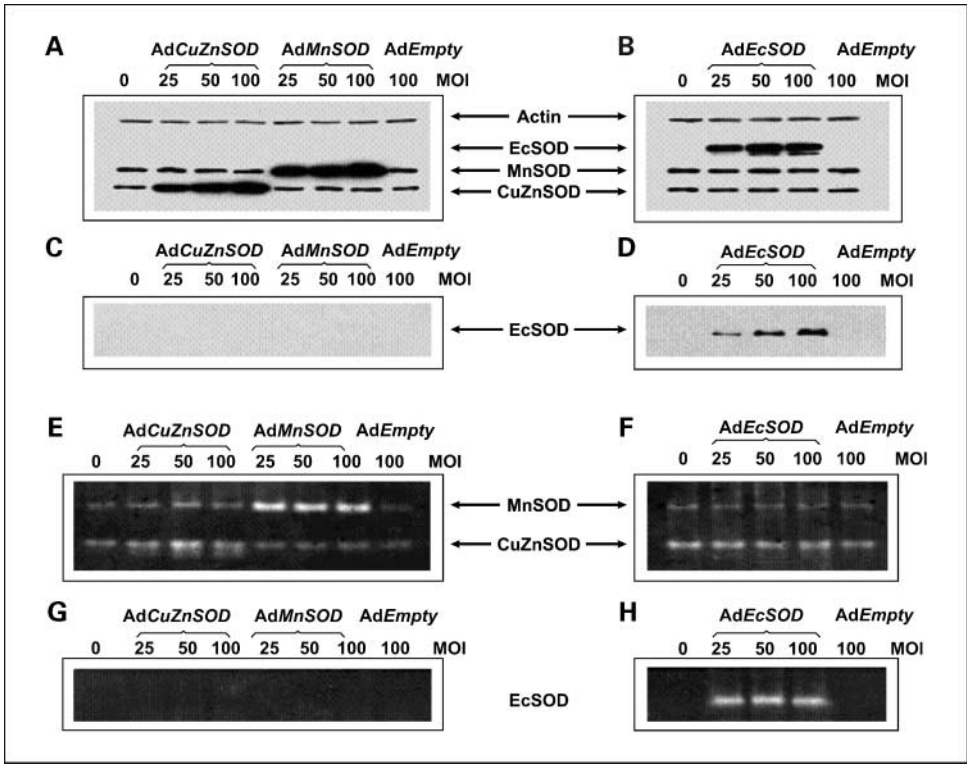

Fig. 1. *A* to *D*, Western blotting analysis showed increases in CuZnSOD, MnSOD, and EcSOD immunoreactivity of adenoviral infected MIA PaCa-2 pancreatic cancer cells with increasing viral titer. MIA PaCa-2 cells were transfected with 100 MOI of Ad*Empty* as a negative control or 0 to 100 MOI of Ad*CuZnSOD*, Ad*MnSOD*, or Ad*EcSOD* as indicated. After 48 h of transfection, total cell lysate was prepared and immunoblotted for the proteins with cellular actin as a loading control (*A* and *B*). Total protein was electrophoresed in a 12.5% SDS-polyacrylamide running gel and a 5% stacking gel. After blocking in 20% fetal bovine serum for 1 h, the sheets were washed and then treated with antibodies to MnSOD, CuZnSOD, or EcSOD. Because EcSOD is secreted into the extracellular space, transduced cell culture medium was immunoblotted to show the presence of EcSOD, but not MnSOD or CuZnSOD, in the media (*C* and *D*). *E* to *H*, SOD enzymatic activities of adenoviral infected MIA PaCa-2 cells. Total cell lysate was also assayed for SOD activities showing increases in both the CuZnSOD and MnSOD activities with increasing viral titer but not EcSOD (*E* and *F*). Proteins (250 μg each) were separated on native polyacrylamide gels and stained for MnSOD activity by the photo-induced nitroblue tetrazolium reaction with 0.75 mmol/L sodium cyanide. EcSOD activity was not detected in cell lysates (*G*). Secreted proteins in transduced cell culture media showed distinctive EcSOD activity bands (*H*), which were not detected in cells infected with Ad*CuZnSOD*, Ad*MnSOD*, or Ad*Empty* or in the parental cell culture media (*G*).

Statistical analysis. Statistical analysis for the *in vitro* studies was done using SYSTAT. A single-factor ANOVA followed by post hoc Tukey test was used to determine statistical differences between means. All means were calculated from three experiments and error bars represent SE. All Western blots, activity assays, and activity gel assays were repeated at least twice. For the *in vivo* studies, the statistical analyses focused on the effects of different treatments on cancer progression. The primary outcomes of interest were time to death and tumor growth over time. Once tumors were visible, the mice were then randomly assigned to a treatment group and followed until death or until the experiment was terminated. If a death was not observed, the mouse was considered lost to follow-up. The log-rank test was used to compare the survival times between treatment groups. Kaplan-Meier survival plots were constructed to estimate survival. Tumor sizes (mm^3) were measured throughout the experiments, resulting in repeated measurements across time for each mouse. Linear mixed-effects regression models were used to estimate and compare the group-specific tumor growth curves. In both the survival and growth curve analyses, statistically significant global tests of equality across groups were followed up with pairwise comparisons to identify specific group differences. All tests were two sided and carried out at the 5% level of significance. Analyses were done with the SAS and R statistical software package.

Results

Adenovirus *SOD* gene transfer greatly increased SOD immunoreactive protein and enzyme activity in MIA PaCa-2 cells

Western blot analysis. To determine whether scavenging superoxide in MIA PaCa-2 cells would inhibit growth, we first overexpressed CuZnSOD, MnSOD, and EcSOD using adenoviral constructs (Ad*CuZnSOD*, Ad*MnSOD*, and Ad*EcSOD*, respectively) at MOIs of 25, 50, and 100. As a negative control for virus infection, adenovirus construct with an empty vector (Ad*Empty*) was used. In MIA PaCa-2 human pancreatic cancer cells, a dose-dependent increase in MnSOD, CuZnSOD, and EcSOD protein immunoreactivity was observed in cells infected with the Ad*MnSOD*, Ad*CuZnSOD*, and Ad*EcSOD* constructs, respectively (Fig. 1A-D). Basal levels of MnSOD and CuZnSOD immunoreactivities were detectable in the parental and 100 MOI Ad*Empty*–infected cells. Control and Ad*Empty*-infected cells did not express EcSOD (Fig. 1A) and infection with Ad*CuZnSOD* and Ad*MnSOD* did not lead to increases in EcSOD protein (Fig. 1C). There was an increase in immunoreactive protein (presumably EcSOD) in cells

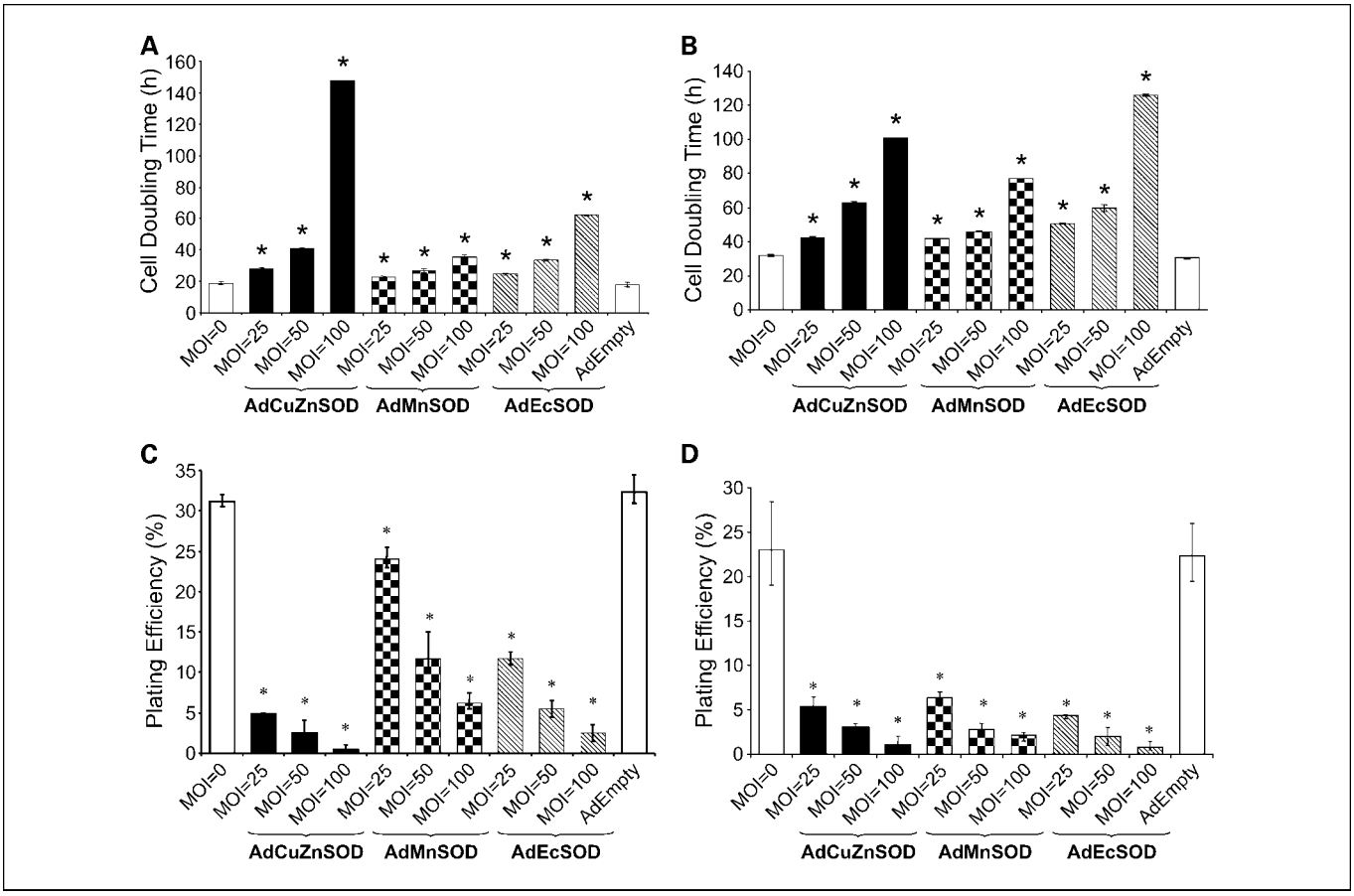

Fig. 2. *In vitro* cancer cell line growth. *A*, doubling times in MIA PaCa-2 pancreatic cancer cell line after overexpression of Ad*MnSOD*, Ad*CuZnSOD*, Ad*EcSOD* (0, 25, 50, and 100 MOI), or Ad*Empty* (100 MOI). Cells infected with Ad*CuZnSOD* had the greatest increases in doubling time compared with the other adenoviral vectors. Columns, mean of three separate experiments ($n = 3$); bars, SE. *, $P < 0.05$, versus 100 MOI Ad*Empty*. *B*, doubling times in BxPC-3 pancreatic cancer cell line after overexpression of Ad*MnSOD*, Ad*CuZnSOD*, Ad*EcSOD* (0, 25, 50, and 100 MOI), or Ad*Empty* (100 MOI). Cells infected with Ad*EcSOD* had the greatest increases in doubling time compared with the other adenoviral vectors. Columns, mean of three separate experiments ($n = 3$); bars, SE. *, $P < 0.05$, versus 100 MOI Ad*Empty*. *C*, plating efficiency. MIA PaCa-2 cells infected with 25, 50, and 100 MOI of Ad*MnSOD*, Ad*CuZnSOD*, or Ad*EcSOD* showed significant reductions in plating efficiency. No significant changes were seen with 100 MOI Ad*Empty* transfer compared with parental cells. Columns, mean plating efficiencies of Ad*MnSOD*-, Ad*CuZnSOD*-, and Ad*EcSOD*- or Ad*Empty*-transduced MIA PaCa-2 cells ($n = 3$); bars, SE. *, $P < 0.05$, versus Ad*Empty*. *D*, BxPC-3 cells infected with 25, 50, and 100 MOI of Ad*MnSOD*, Ad*CuZnSOD*, or Ad*EcSOD* showed significant reductions in plating efficiency. No significant changes were seen with 100 MOI Ad*Empty* transfer compared with parental cells. Columns, mean plating efficiencies of Ad*MnSOD*-, Ad*CuZnSOD*-, and Ad*EcSOD*- or Ad*Empty*-transduced MIA PaCa-2 cells ($n = 3$); bars, SE. *, $P < 0.05$, versus Ad*Empty*.

infected with the Ad*EcSOD* vector without an increase in either MnSOD or CuZnSOD protein (Fig. 1B). Because EcSOD is an extracellular protein, we also determined the presence of the protein in the culture media and found that there was also increased immunoreactive protein in media of cells infected with Ad*EcSOD* (Fig. 1D) but not Ad*CuZnSOD* or Ad*MnSOD* (Fig. 1C).

As seen with the immunoreactive protein, there was a dose-dependent increase in MnSOD and CuZnSOD activity in cells infected with the Ad*MnSOD* and Ad*CuZnSOD* constructs, respectively (Fig. 1E). MnSOD and CuZnSOD activities were detectable in the parental and 100 MOI Ad*Empty* – infected cells. There was no increase in MnSOD or CuZnSOD activity in cells infected with the Ad*EcSOD* vector (Fig. 1F), and there was no detectable EcSOD activity after infection with the Ad*CuZnSOD* or Ad*MnSOD* vectors (Fig. 1G). Although EcSOD protein was detected from the Ad*EcSOD*-infected cell lysate (Fig. 1B), its activity was undetectable in the same sample from the activity gel assay. In fact, there was only increased activity in media in cells infected with Ad*EcSOD* (Fig. 1H). These data indicate that in MIA PaCa-2 cells, protein level and enzymatic activities of all of the SODs (MnSOD, CuZnSOD, and EcSOD) were increased to a similar extent with the adenoviral transduction.

Tumor biological characteristics of adenovirus-transduced cells change with increasing MOI

Cell growth. Tumor cell growth characteristics were used to evaluate the effect of the overexpression of MnSOD, CuZnSOD, and EcSOD in cell culture. The growth rate, cell population doubling time, and plating efficiency were therefore examined and the data represent the mean of three separate experiments. MIA PaCa-2 human pancreatic cancer cells infected with Ad*MnSOD*, Ad*CuZnSOD*, and Ad*EcSOD* showed slower *in vitro* growth compared with parental cells and cells infected with the Ad*Empty* vector (Fig. 2A). MIA PaCa-2 cell growth significantly decreased with Ad*MnSOD* (25, 50, and 100 MOI) when compared with the parental cells or 100 MOI Ad*Empty* cells. For example, on day 6, cell number decreased by >17-fold with the 100 MOI Ad*MnSOD* – infected cells compared with 100 MOI Ad*Empty* (Fig. 2A). Ad*EcSOD* (25, 50, and 100 MOI) also had significant effects in decreasing MIA PaCa-2 cell growth significantly when compared with the parental cells or 100 MOI Ad*Empty* cells. For example, on day 6, cell number decreased by 84-fold with the 100 MOI Ad*EcSOD* compared with 100 MOI Ad*Empty* (Fig. 2A). Ad*CuZnSOD* (25, 50, and 100 MOI) had the greatest effects in inhibiting MIA PaCa-2 cell growth significantly when compared with the parental cells or 100 MOI Ad*Empty* cells. On day 6, cell number decreased by >125-fold with the 100 MOI Ad*CuZnSOD* – infected cells compared with 100 MOI Ad*Empty* (Fig. 2A). When comparing the results from the three separate adenoviral constructs containing the three different SODs, doubling time was greatest in the MIA PaCa-2 cells that were infected with the Ad*CuZnSOD* vector (Fig. 2A). Doubling time in cells infected with the Ad*Empty* vector was 18.2 ± 1.5 h (means ± SE; $n = 3$). Doubling time was 147 ± 0.4 h after Ad*CuZnSOD* 100 MOI treatment, which was significantly greater than Ad*MnSOD* 100 MOI (36 ± 0.9 h) and Ad*EcSOD* 100 MOI (62 ± 0.7 h; mean ± SE; $n = 3$; $P < 0.05$).

SOD overexpression in another pancreatic cancer cell line, BxPC-3, showed similar inhibition of *in vitro* growth (Fig. 2B). Infection with Ad*MnSOD*, Ad*CuZnSOD*, or Ad*EcSOD* all inhibited cell growth at adenoviral titers of 25 to 100 MOI compared with the Ad*Empty* vector at 100 MOI. However, in the BxPC-3 cell line, Ad*EcSOD* 100 MOI had a greater effect in inhibiting growth (doubling time of 126 h) compared with Ad*MnSOD* 100 MOI (doubling time of 76 h) and Ad*CuZnSOD* 100 MOI (doubling time of 100 h).

Plating efficiency. To determine the clonogenic capacity of adenoviral infected cells, we carried out a plating efficiency assay. In general, malignant cells have a higher plating efficiency than do normal cells. MIA PaCa-2 cells treated with

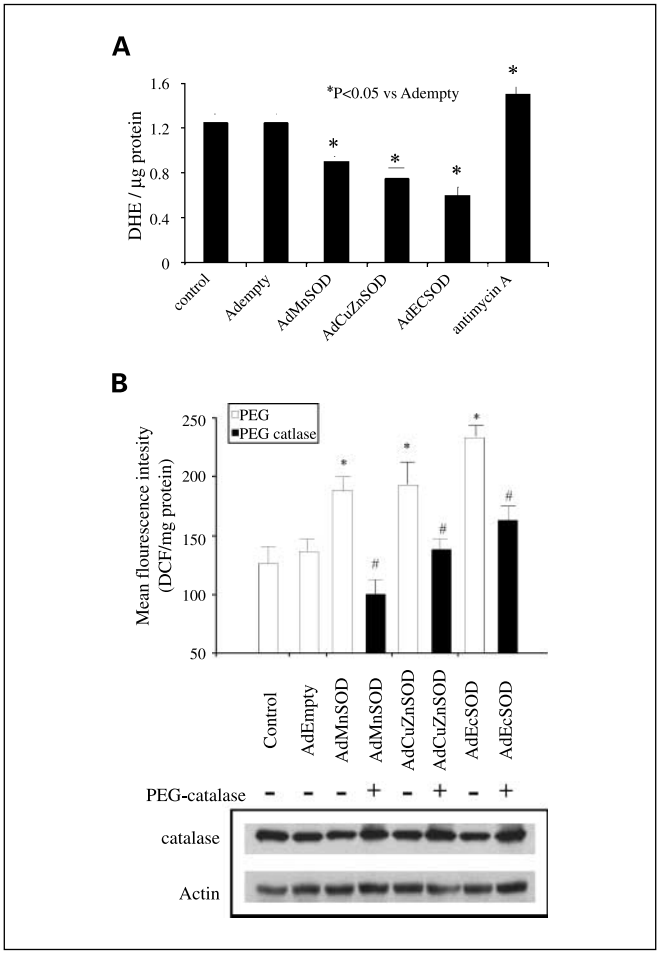

Fig. 3. *A*, intracellular hydroethidine fluorescence decreased in MIA PaCa-2 cells infected with Ad*MnSOD*, Ad*CuZnSOD*, or Ad*EcSOD*. Intracellular superoxide levels as measured by dihydroethidium (*DHE*) decreased significantly 48 h after infection with Ad*MnSOD*, Ad*CuZnSOD*, or Ad*EcSOD* 100 MOI compared with control MIA PaCa-2 pancreatic carcinoma cells or the same cells infected with the Ad*Empty* vector. As a positive control, antimycin A, a known inhibitor of complex III in the mitochondrial electron transport chain, results in significantly increased superoxide levels. *, $P < 0.05$, versus Ad*Empty*. Columns, mean ($n = 3$); bars, SE. *B*, intracellular DCFH fluorescence increased in MIA PaCa-2 cells infected with Ad*MnSOD*, Ad*CuZnSOD*, or Ad*EcSOD*. Intracellular peroxide levels as measured at 96 h by DCFH increased >2- to 2.5-fold after infection with Ad*MnSOD*, Ad*CuZnSOD*, or Ad*EcSOD* 100 MOI compared with control MIA PaCa-2 pancreatic carcinoma cells or the same cells infected with the Ad*Empty* vector. To determine if increases in fluorescence of DCFH were due to hydrogen peroxide, cells were also treated with PEGylated catalase (PEG-catalase; Sigma). Western blotting showed an increase in catalase immunoreactivity in cells treated with PEGylated catalase (100 units/mL). The increased intracellular DCFH fluorescence in MIA PaCa-2 cells infected with Ad*MnSOD*, Ad*CuZnSOD*, or Ad*EcSOD* was reversed when cells were treated with the same adenoviral vectors and with PEG-catalase. *, $P < 0.05$, versus Ad*Empty*; #, $P < 0.05$, versus PEG alone groups. Columns, mean ($n = 3$); bars, SE.

the Ad*CuZnSOD* vector had the greatest reduction in plating efficiency (Fig. 2C). Plating efficiency was reduced to 32.0 ± 1.3% and 31.2 ± 0.8% in the Ad*Empty* 100 MOI and control groups (0 MOI), respectively. Enforced expression of Ad*MnSOD* decreased plating efficiency in a dose-dependent manner with the 100 MOI dose decreasing the plating efficiency to 6.2 ± 2.2%. Infection with Ad*EcSOD* also decreased the plating efficiency in a dose-dependent manner to a plating efficiency of 2.5 ± 1.0% at 100 MOI. Ad*CuZnSOD* decreased plating efficiency most significantly to 4.8 ± 0.2%, 2.5 ± 1.5%, and 0.4 ± 0.6% at the 25, 50, and 100 MOI doses, respectively ($P < 0.01$, versus Ad*Empty* and controls). Overexpression of the

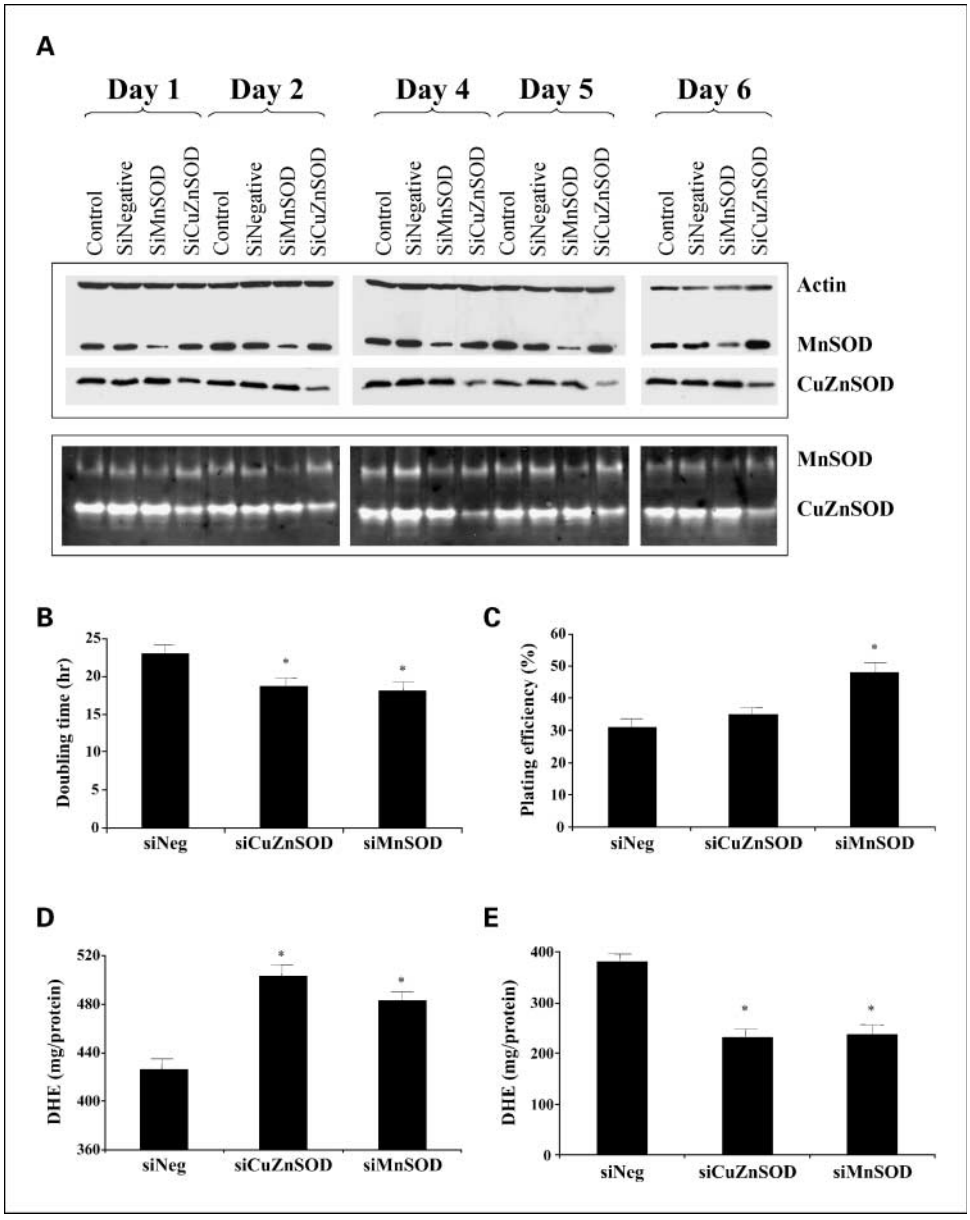

Fig. 4. Inhibition of MnSOD and CuZnSOD in MIA PaCa-2 with siRNAs. After 48 h of transfection with specific siRNAs for MnSOD and CuZnSOD using LipofectAMINE transfection reagent, cells were trypsinized and seeded at a density of 5×10^3 per well in a 24-well plate. Growth rates of cells were then analyzed at different time points as indicated, with day 1 corresponding to 48 h after siRNA transfection. At the same time points, another set of cells were also harvested for Western blotting, SOD activity gels, cell growth, plating efficiency, hydroethidine fluorescence, and DCFH fluorescence. *A*, top, Western blot analysis showing a time course inhibition of MnSOD and CuZnSOD protein levels with cellular actin used as a loading control. Both SODs were inhibited by at least 50% in comparison with the control and the siNeg-transfected samples from day 2 to day 8 after transfection. Bottom, SOD activity gels showing the corresponding inhibition of SOD activities by the siRNA at different time points. The siRNAs used were able to reduce both the endogenous protein levels as well as enzymatic activities of MnSOD and CuZnSOD. *B*, doubling time. At the same time point as indicated in *A*, infected cells were counted for growth rate comparison and cell doubling time was determined. In comparison with the siNeg-transfected cell, which has a doubling time of 22.2 h, inhibition of MnSOD shortened the doubling time to 18.1 h whereas siCuZnSOD-transfected cells had a doubling time of 18.7 h. *, $P < 0.05$, versus siNeg. Columns, mean ($n = 3$); bars, SE. *C*, plating efficiency. Inhibition of either MnSOD or CuZnSOD increased the plating efficiency of MIA PaCa-2 cells from 31.5 ± 3.0% in siNeg-transfected sample to 48.5 ± 3.5% in siMnSOD-transfected sample and 35 ± 2.2% in siCuZnSOD-transfected sample. *, $P < 0.05$, siNeg versus siMnSOD. Columns, mean ($n = 3$); bars, SE. *D*, intracellular hydroethidine fluorescence increases in MIA PaCa-2 cells treated with siCuZnSOD and siMnSOD when compared with siNeg. Columns, mean ($n = 3$); bars, SE. *, $P < 0.05$, versus siNeg. *E*, intracellular DCFH fluorescence decreases in MIA PaCa-2 cells treated with siCuZnSOD and siMnSOD when compared with siNeg. Columns, mean ($n = 3$); bars, SE. *, $P < 0.05$, versus siNeg.

SODs also decreased plating efficiency in the BxPC-3 cell line (Fig. 2D). Unlike the MIA PaCa-2 cell line where Ad*CuZnSOD* had the greatest decrease in plating efficiency, in the BxPC-3 cell line, all of the adenoviral vectors had very similar decreases in plating efficiency at similar MOIs.

To determine the apoptotic and necrotic populations of cells, MIA PaCa-2 cells were infected with the adenovirus constructs at 100 MOI and incubated with Annexin and propidium iodide. Fluorescence-activated cell sorting analysis showed that there were no differences in the percentage of cells staining for Annexin-propidium iodide after infection with 100 MOI of Ad*Empty*, Ad*CuZnSOD*, Ad*EcSOD*, or Ad*MnSOD* (data not shown); this shows that significant killing is not observed with the three forms of SOD compared with Ad*Empty*.

SOD overexpression alters ROS levels

If the antioxidant enzymes MnSOD, EcSOD, and CuZnSOD inhibit growth of pancreatic cancer by scavenging of superoxide, then we should be able to see a decrease in superoxide levels after overexpression of these antioxidant enzymes and an increase in hydrogen peroxide levels (22). Intracellular generation of O_2^- was assessed by hydroethidine fluorescence and the level of intracellular peroxide was determined with DCFH diacetate. Figure 3A shows that overexpression of MnSOD, CuZnSOD, or EcSOD decreases hydroethidine fluorescence in MIA PaCa-2 pancreatic cancer cells. As a positive control, antimycin A, a known inhibitor of complex III in the mitochondrial electron transport chain, results in significantly increased hydroethidine fluorescence. When compared with MIA PaCa-2 cells treated with the Ad*Empty* vector, hydroethidine fluorescence levels were decreased by 26%, 37%, and 51% with the Ad*MnSOD*, Ad*CuZnSOD*, and Ad*EcSOD* vectors, respectively. In contrast, overexpression of MnSOD, CuZnSOD, or EcSOD resulted in increases in DCFH fluorescence (Fig. 3B). Compared with the Ad*Empty*-infected cells, there were increases in DCFH fluorescence of 21%, 66%, and 92% with the Ad*MnSOD*, Ad*CuZnSOD*, and Ad*EcSOD* vectors, respectively. As mentioned, interaction of DCFH with oxidants such as peroxide gives rise to cellular fluorescence. Because DCFH can also be oxidized by other ROS such as hydroxyl radical, PEGylated catalase was used to show that SOD-induced increases in DCFH fluorescence were most likely due to hydrogen peroxide. As seen in Fig. 3B, PEG-catalase treatment reversed the increase in DCFH fluorescence induced by enforced expression of *MnSOD*, *CuZnSOD*, and *EcSOD*. The reversal of SOD-induced increase in DCFH fluorescence was greatest in the MnSOD group, which may be due to the fact that CuZnSOD is known to back react at a slow rate with H_2O_2, producing a hydroxyl radical–like species (23) that also oxidizes DCFH. Although EcSOD has not been shown to be able to generate hydroxyl radical, it may behave in a similar fashion to CuZnSOD based on the ~50% homology of the two enzymes at the active catalytic site (24).

Inhibition of CuZnSOD and MnSOD alters cell growth and ROS levels

To further determine the role of SOD in scavenging of superoxide and in the growth of pancreatic cancer, siRNAs to CuZnSOD and MnSOD were used (because EcSOD is not naturally expressed in pancreatic cancer cells or media, we could not inhibit this enzyme). Cells were seeded for 24 h and then transfected with 200 pmol of siRNAs (siNeg, siCuZnSOD, or siMnSOD) using LipofectAMINE 2000 (Invitrogen) transfection reagent. Forty-eight hours after transfection, cells were seeded and growth rate was determined. This was considered day 1, and at different time points, as indicated in Fig. 4A, cells were harvested for Western blotting analysis and SOD activity. Western blots and activity gels to CuZnSOD and MnSOD showed that the siRNA constructs decreased CuZnSOD and MnSOD protein and activity by at least 50% in comparison with the control and the siNeg-transfected samples from day 2 to day 8 after transfection (Fig. 4A). The decrease in CuZnSOD and MnSOD protein and activity resulted in faster cell growth as seen by decreased doubling time (Fig. 4B). Additionally, plating efficiency was increased in cells treated with siMnSOD but not siCuZnSOD compared with siNeg (Fig. 4C). The inhibition of CuZnSOD and MnSOD resulted in altered levels

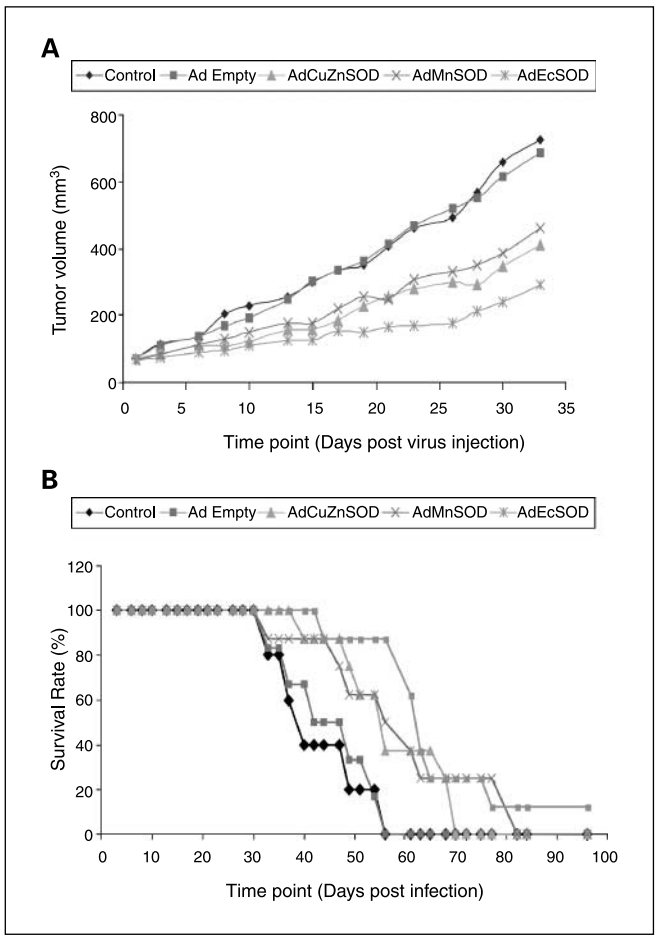

Fig. 5. *A*, Ad*MnSOD*, Ad*CuZnSOD*, or Ad*EcSOD* injections decreased MIA PaCa-2 tumor growth in nude mice. The Ad*EcSOD* group had significantly slower tumor growth when compared with the control and Ad*Empty* ($P < 0.0001$; $n = 5$-8 per group). MIA PaCa-2 tumor cells (2×10^6) were delivered s.c. into the flank region of nude mice. Controls received serum-free media in similar volumes. Ad*MnSOD*, Ad*CuZnSOD*, Ad*EcSOD*, or Ad*Empty* constructs (1×10^9 plaque-forming units) were delivered to the tumor on day 1 of the experiment. On day 33, there was a 3-fold decrease in tumor growth in animals receiving the Ad*EcSOD* vector when compared with treatment with the Ad*Empty* control vector. *B*, Kaplan-Meier plots of estimated survival after injection of MIA PaCa-2 tumors in nude mice. There was a significant difference in survival between Ad*Empty* and Ad*EcSOD* ($P = 0.001$). There were significant differences in survival ($P < 0.05$) between controls and Ad*CuZnSOD*, Ad*MnSOD*, or Ad*EcSOD*.

Table 1. *In vivo* tumor growth over time between treatment groups for the data shown in Fig. 5A

(A) Mixed linear regression models comparing tumor growth between treatment groups

Groups	*n*	Mean tumor size (mm^3)	*P*	Pairwise differences
Controls	96	473.2		Control vs Ad*CuZnSOD*,
Ad*Empty*	121	473.1		Ad*MnSOD*, and Ad*EcSOD*;
Ad*CuZnSOD*	197	384.2	< 0.0001	Ad*Empty* vs Ad*CuZnSOD*,
Ad*MnSOD*	199	401.2		Ad*MnSOD*, and Ad*EcSOD*
Ad*EcSOD*	216	350.6		

(B) *P* values for pairwise group comparisons of the tumor growth curves

Comparison	*P*
Controls vs Ad*Empty*	0.56
Controls vs Ad*CuZnSOD*	0.001
Controls vs Ad*MnSOD*	0.04
Controls vs Ad*EcSOD*	0.01
Ad*Empty* vs Ad*CuZnSOD*	<0.001
Ad*Empty* vs Ad*MnSOD*	0.01
Ad*Empty* vs Ad*EcSOD*	<0.001
Ad*CuZnSOD* vs Ad*MnSOD*	0.01
Ad*CuZnSOD* vs Ad*EcSOD*	0.11
Ad*MnSOD* vs Ad*EcSOD*	0.16

NOTE: The sample sizes (*n*) given in the table are the total number of measurements available within each group. The *P* values are for the global tests of equality between the growth curves across treatment groups.

of hydroethidine and DCFH fluorescence. In MIA PaCa-2 cells treated with siCuZnSOD or siMnSOD, hydroethidine fluorescence was increased (Fig. 4D). Moreover, DCFH fluorescence was decreased in cells treated with either siCuZnSOD or siMnSOD (Fig. 4E).

Growth of tumor xenografts

To test the hypothesis that besides MnSOD, CuZnSOD and EcSOD could reduce tumor growth *in vivo*, we injected 2×10^6 MIA PaCa-2 cells s.c. into the flank region of nude mice and allowed tumors to reach 4 × 5 mm in greatest dimension. The adenovirus constructs were then injected into the tumors and the tumor volume was followed over time until they reached 1,000 mm^3, at which the mice were sacrificed. The Ad*Empty* vector was used to determine the role of adenovirus infection by itself on tumor suppression. When the Ad*MnSOD* construct was given, a slower growth in tumor was observed in comparison with the control group as well as the Ad*Empty* injected group (Fig. 5A). The control and the Ad*Empty* group had mean tumor volumes of 473 and 473 mm^3, respectively, whereas the Ad*MnSOD* group had a mean tumor volume of 401 mm^3 (Table 1A). This result is not surprising because previous work has shown similar tumor-suppressive effects of Ad*MnSOD* (19). However, the Ad*CuZnSOD* group had even more tumor growth suppression than the Ad*MnSOD* group, with a mean tumor volume of 384 mm^3. Surprisingly, animals that received Ad*EcSOD* had the smallest tumor volumes (350 mm^3) among the groups.

The mixed linear regression analysis of the tumor growth curves showed that their rate of growth differed significantly between the groups ($P < 0.0001$; Table 1A). Pairwise group comparisons were carried out to identify where the group differences occurred. The group pairs for which significant differences were observed included controls versus Ad*MnSOD*, Ad*CuZnSOD*, and Ad*EcSOD* ($P < 0.05$) and Ad*Empty* versus Ad*MnSOD*, Ad*CuZnSOD*, and Ad*EcSOD* ($P < 0.05$; Table 1B). The only nonsignificant group differences were between controls and mice that received the Ad*Empty* construct, between the groups of mice that received the Ad*CuZnSOD* and Ad*EcSOD* treatments, and between the Ad*MnSOD* and Ad*EcSOD* groups. Estimated tumor growth curves are displayed in Fig. 5A. Metastases are rare in this heterotopic model of pancreatic cancer, yet they do occur (25). In addition, some investigators have suggested that MnSOD-dependent generation of H_2O_2 leads to increased expression of matrix metalloproteinase-1 and to enhanced invasive capacity of tumors with elevated levels of MnSOD (26, 27). None of the animals in this current study developed metastatic disease.

The estimated survival curves for each treatment group are given in the Kaplan-Meier plots of Fig. 5B. The log-rank analyses of survival showed that the animals that received Ad*MnSOD* had increased survival compared with controls (58.5 versus 40.0 days), whereas the Ad*Empty* group had a mean survival rate of 45.5 days. Again, Ad*EcSOD* group had the highest survival rate among the treatment group (63 days) whereas animals with Ad*CuZnSOD* treatment had a survival rate of 56 days (Table 2A). The global test of equality indicates that there is a significant difference in the survival times ($P = 0.003$). Pairwise group comparisons were carried out to identify where the group differences occurred. The group of animals that received the Ad*EcSOD* vector had significant increases in survival when compared with the control and Ad*Empty* groups ($P = 0.001$; Table 2B). Ad*CuZnSOD* and Ad*MnSOD* both had significant increases in survival when compared with controls ($P = 0.02$, $P = 0.04$, respectively) and approached statistical significance when compared with Ad*Empty* ($P = 0.05$ and $P = 0.07$, respectively). No significant

differences were observed between the control and Ad*Empty* groups, the Ad*Empty*, Ad*CuZnSOD*, and Ad*MnSOD* groups, and the Ad*CuZnSOD*, Ad*MnSOD*, and Ad*EcSOD* groups.

Discussion

Our present study shows that SOD-mediated modulation of ROS influences the malignant phenotype of pancreatic cancer. Increases in SOD immunoreactivity and activity were seen after infections with the Ad*MnSOD*, Ad*CuZnSOD*, or Ad*EcSOD* constructs. Increased SOD activity decreased hydroethidine fluorescence and increased DCFH fluorescence. Increasing SOD levels correlated with increased doubling time. Cell growth and plating efficiency decreased with increasing amounts of the adenoviral constructs, with the Ad*CuZnSOD* having the greatest effect in decreasing *in vitro* tumor growth. Conversely, inhibition of MnSOD and CuZnSOD with siRNA resulted in increased superoxide levels and faster cell growth. Tumors grew slower and survival was increased in nude mice injected with the Ad*MnSOD*, Ad*CuZnSOD*, or Ad*EcSOD* constructs when compared with Ad*Empty*.

As with most other solid tumors, primary pancreatic cancers have been shown to have low levels of antioxidant enzymes (28). Immunohistochemistry showed that MnSOD, CuZnSOD, catalase, and glutathione peroxidase immunoreactive protein levels are decreased in human pancreatic ductal carcinoma specimens when compared with normal human pancreas (29). Similar findings are seen in primary pancreatic cancer cell lines, including the pancreatic cancer cell line MIA PaCa-2, which has decreased levels of MnSOD immunoreactivity and enzyme activity when compared with normal human pancreas (18). In that study, the levels of EcSOD immunoreactive protein or activity were not assessed. Our current study showed that EcSOD immunoreactivity was absent in pancreatic cancer cells. Our previous studies showed that all pancreatic cancer cell lines studied had variable levels of CuZnSOD whereas cell doubling time was most rapid in the cell lines with the lowest levels of MnSOD. There was no correlation between cell growth and the levels of other antioxidant enzymes, whereas MnSOD activity and immunoreactive protein correlated with pancreatic tumor cell doubling time. Our previous studies suggested that MnSOD may play a role in the growth of pancreatic cancer *in vitro* and that MnSOD may be effective in tumor growth suppression in this devastating disease. We expanded these studies and showed that overexpression of MnSOD in both cell culture and direct injection of Ad*MnSOD* into preestablished tumor xenografts inhibited pancreatic tumor growth (19). Our current study showed the same findings with MnSOD overexpression but clearly showed that the other SODs, CuZnSOD and EcSOD, may be even more effective in growth inhibition. Similar findings have recently been shown in breast cancer cells. Enforced expression of MnSOD or CuZnSOD by adenoviral infections resulted in equivalent tumor suppression in various breast cancer cell lines (29). In our current study, CuZnSOD had greater *in vitro* tumor suppression in pancreatic cancer cells whereas EcSOD had greater *in vivo* tumor suppression in pancreatic tumors, suggesting that plasma membrane–generated or extracellular superoxide may play a bigger role in the growth of pancreatic cancers.

Our study correlates well with other investigations applying siRNA to inhibit endogenous levels of SOD. Hu et al. (30) have shown that inhibition of MnSOD in ovarian cancer cells by siRNA led to cell proliferation *in vitro*, increases in superoxide levels, and greater tumor growth *in vivo*. Our current study shows a similar effect with MnSOD and further shows that inhibition of CuZnSOD also increases cell growth and increases hydroethidine fluorescence. Taken together, these studies

Table 2. *In vivo* survival over time between treatment groups for the data shown in Fig. 5B

(A) Log-rank tests comparing the median survival times between treatment groups

Groups	*n*	Median survival	*P*	Pairwise differences
Controls	5	40.0		Controls vs Ad*CuZnSOD*,
Ad*Empty*	6	45.5		Ad*MnSOD*, and Ad*EcSOD*;
Ad*CuZnSOD*	8	56.0	0.003	Ad*Empty* vs Ad*CuZnSOD*,
Ad*MnSOD*	8	58.5		and Ad*EcSOD*
Ad*EcSOD*	8	63.0		

(B) *P* values for pairwise group comparisons of survival

Comparison	*P*
Controls vs Ad*Empty*	0.62
Controls vs Ad*CuZnSOD*	0.02
Controls vs Ad*MnSOD*	0.04
Controls vs Ad*EcSOD*	0.001
Ad*Empty* vs Ad*CuZnSOD*	0.05
Ad*Empty* vs Ad*MnSOD*	0.07
Ad*Empty* vs Ad*EcSOD*	0.001
Ad*CuZnSOD* vs Ad*MnSOD*	0.67
Ad*CuZnSOD* vs Ad*EcSOD*	0.33
Ad*MnSOD* vs Ad*EcSOD*	0.48

NOTE: *P* values are for global tests of equality across groups.

suggest that the prooxidant environment leads to cell proliferation and reinforces the importance of ROS regulation of cellular homeostasis.

Mounting evidence suggests that increases in steady-state levels of ROS may trigger transformation and contribute to cancer progression by amplifying genomic instability (31). Our current study adds further data to suggest that generated ROS leads to pancreatic cancer cell proliferation and correlates well with others showing that ROS are prosurvival factors in pancreatic cancer (5). We and others (5) have shown that inhibiting ROS by different approaches inhibits growth in pancreatic cancer cells. Vaquero et al. (5) inhibited ROS using various antioxidants including Tiron and *N*-acetylcysteine, MnSOD plasmid transfection, and Nox4 antisense. Their study shows that ROS protect pancreatic cancer cells from apoptosis. Thus, the prosurvival effect of ROS may be an important mechanism of pancreatic cancer cell resistance to therapy and reducing ROS may be a rational therapeutic approach. The opposite strategy of increasing ROS levels may also be a valid approach. Trachootham et al. (32) used this approach in ovarian epithelial cells expressing *H-Ras*^{V12} treated with β-phenylethyl isothiocyanate, which effectively disables the glutathione antioxidant system and causes severe ROS accumulation preferentially in the transformed cells due to increases in ROS. Our group has also used similar approaches with dicumarol, a naturally occurring anticoagulant that increases mitochondrial production of ROS and preferential cytotoxicity to transformed cell lines (33).

In summary, we have shown that overexpression of MnSOD, CuZnSOD, and EcSOD decreases superoxide levels and increases peroxide levels in pancreatic tumor cells. Increasing SOD levels correlated with slower *in vitro* growth. Overexpression of CuZnSOD had the greatest effect *in vitro* in inhibiting cell growth and plating efficiency, whereas direct injections of the Ad*EcSOD* vector had the greatest effect in inhibiting *in vivo* tumor growth and increasing survival. These studies suggest that scavenging membrane-generated superoxide may have beneficial effects on pancreatic cancer treatments.

Acknowledgments

We thank Yuping Zhang for technical support and Dr. Donald Heistad (Department of Internal Medicine, University of Iowa, Iowa City, Iowa) for providing the EcSOD antibody.

References

1. Jemal A, Siegel R, Ward E, Murray T, Xu J, Thun M. Cancer statistics, 2007. CA Cancer J Clin 2007;57:43–66.
2. Motojima K, Urano T, Nagata Y, Shiku H, Tsurifune T, Kanematsu T. Detection of point mutations in the Kirsten-ras oncogene provides evidence for the multicentricity of pancreatic carcinoma. Ann Surg 1993;217:138–43.
3. Motojima K, Tsunoda T, Kanematsu T, Nagata Y, Urano T, Shiku H. Distinguishing pancreatic carcinoma from other periampullary carcinomas by analysis of mutations in the Kirsten-ras oncogene. Ann Surg 1991;214:657–62.
4. Rivera J, Werner J, Adrie C, Rattner DW. Analysis of *K-ras* oncogene mutations in chronic pancreatitis with ductal hyperplasia. Surgery 1997;121:42–9.
5. Vaquero EC, Edderkaoui M, Pandol SJ, Gukovsky I, Gukovskaya AS. Reactive oxygen species produced by NAD(P)H oxidase inhibit apoptosis in pancreatic cancer cells. J Biol Chem 2004;279:34643–54.
6. Santillo M, Mondola P, Seru R, et al. Opposing functions of Ki- and Ha-*Ras* genes in the regulation of redox signals. Curr Biol 2001;11:614–9.
7. Irani K, Xia Y, Zweier JL, et al. Mitogenic signaling mediated by oxidants in Ras-transformed fibroblasts. Science 1997;275:1649–51.
8. Yang J-Q Li S, Domann FE, Buettner GR, Oberley LW. Superoxide generation in v-Ha-ras-transduced human keratinocyte HaCaT cells. Mol Carcinog 1999;26:180–8.
9. Oberley LW, Oberley TD. Free radicals, cancer, and aging. In: Johnson JE, Jr., Walford R, Harmon D, Miquel J, editors. Free radicals, aging, and degenerative diseases. Alan R. Liss, Inc.; 1986. p. 325–81.
10. Crapo JD, Oury T, Rabouille C, Slot JW, Chang LY. Copper zinc superoxide dismutase is primarily a cytosolic protein in human cells. Proc Natl Acad Sci U S A 1992;89:10405–9.
11. Okado-Matsumoto A, Fridovich I. Subcellular distribution of superoxide dismutases (SOD) in rat liver: Cu Zn-SOD in mitochondria. J Biol Chem 2001;276:38388–93.
12. Sturtz LA, Diekert K, Jensen LT, Lill R, Culotta VC. A fraction of yeast Cu Zn-superoxide dismutase and its metallochaperone, CCS, localize to the intermembrane space of mitochondria. A physiological role for SOD1 in guarding against mitochondrial oxidative damage. J Biol Chem 2001;276:38084–9.
13. Marklund SL, Holme E, Hellner L. Superoxide dismutase in extracellular fluids. Clin Chim Acta 1982;126:41–51.
14. Marklund S. Human copper-containing superoxide dismutase of high molecular weight. Proc Natl Acad Sci U S A 1982;79:7634–8.
15. Wheeler MD, Smutney OM, Samulski RJ. Secretion of extracellular superoxide dismutase from muscle transduced with recombinant adenovirus inhibits the growth of B16 melanomas in mice. Mol Cancer Res 2003;1:871–81.
16. Sandstrom J, Carlsson L, Marklund SL, Edlund T. The heparin-binding domain of extracellular superoxide dismutase C and formation of variants with reduced heparin affinity. J Biol Chem 1992;267:18205–9.
17. Weisiger RA, Fridovich I. Mitochondrial superoxide dismutase: site of synthesis and intramitochondrial localization. J Biol Chem 1973;248:4793–6.
18. Cullen JJ, Weydert C, Hinkhouse MM, et al. The role of manganese superoxide dismutase in the growth of pancreatic adenocarcinoma. Cancer Res 2003;63:1297–303.
19. Wydert C, Roling B, Liu J, Ritchie JM, Oberley LW, Cullen JJ. Suppression of the malignant phenotype in human pancreatic cancer cells by the overexpression of manganese superoxide dismutase. Mol Cancer Ther 2003;2:361–9.
20. Davis BJ. Disc electrophoresis-II. Method and application to human serum proteins. Ann N Y Acad Sci 1964;121:404–27.
21. Beauchamp C, Fridovich I. Superoxide dismutase: improved assays and an assay applicable to acrylamide gels. Anal Biochem 1971;44:276–87.
22. Buettner GR, Ng CF, Wang M, Rodgers VGJ, Schafer FQ. A new paradigm: manganese superoxide dismutase influences the production of H_2O_2 and thereby their biological state. Free Radic Biol Med 2006;42:1338–50.
23. Valentine JS. Do oxidatively modified proteins cause ALS? Free Radic Biol Med 2002;33:1314–20.
24. Hjalmarsson K, Marklund SL, Engstrom A, Edlund T. Isolation and sequence of complementary DNA encoding human extracellular superoxide dismutase. Proc Natl Acad Sci U S A 1987;84:6340–4.
25. Lewis A, Du J, Liu J, Ritchie JM, Oberley LW, Cullen JJ. Metastatic progression of pancreatic cancer: changes in antioxidant enzymes and cell growth. Clin Exp Metastasis 2006;22:523–32.
26. Ranganathan AC, Nelson KK, Rodriguez AM, et al. Manganese superoxide dismutase signals matrix metalloproteinase expression via H2O2-dependent ERK1/2 activation. J Biol Chem 2001;276:14264–720.
27. Nelson KK, Ranganathan AC, Mansouri J, et al. Elevated Sod2 activity augments matrix metalloproteinase expression: evidence for the involvement of endogenous hydrogen peroxide in regulating metastasis. Clin Cancer Res 2003;9:424–32.
28. Cullen JJ, Mitros FA, Oberley LW. Expression of antioxidant enzymes in diseases of the human pancreas: another link between chronic pancreatitis and pancreatic cancer. Pancreas 2003;26:23–7.
29. Weydert CJ, Waugh TA, Ritchie JM, et al. Over expression of manganese or copper-zinc superoxide dismutase inhibits breast cancer growth. Free Radic Biol Med 2006;41:226–37.
30. Hu Y, Rosen DG, Zhou Y, et al. Mitochondrial manganese-superoxide dismutase expression in ovarian cancer: role in cell proliferation and response to oxidative stress. J Biol Chem 2005;280:39485–92.
31. Schumacker PT. Reactive oxygen species in cancer cells: live by the sword, die by the sword. Cancer Cell 2006;10:175–6.
32. Trachootham D, Zhou Y, Zhang H, et al. Selective killing of oncogenically transformed cells through a ROS-mediated mechanism by β-phenylethyl isothiocyanate. Cancer Cell 2006;10:241–52.
33. Du J, Daniels DH, Asbury C, et al. Mitochondrial production of reactive oxygen species mediate dicumarol-induced cytotoxicity in cancer cells. J Biol Chem 2006;281:37416–26.